ed and observed phases of the diurnal component. Although the model appears to consistently overestimate the diurnal amplitude, it does closely follow the observed trends in amplitude. Furthermore, the model simulation of the semidiurnal surface pressure oscillation is remarkably good.

Considering both the simplifications used in the theory and the limitation of the data to only two sites, the overall agreement is surprisingly good. The classical atmospheric tidal theory used here was originally developed to explain the daily variations in surface pressure observed for the earth's atmosphere (*8*). Application of this theory to Mars was thought to be limited primarily by the effects of the martian relief (*10*). The present results demonstrate that the classical theory can simulate major features of the martian atmospheric tides during a great dust storm and that, in doing so, a reliable measure of the planet-wide opacity due to airborne dust can be inferred from the semidiurnal tide at VL1. Application of this technique to the second martian year of VL1 data reveals a less intense event (1979a) corresponding to the 1977a storm, but no opacity comparable to the second, more intense 1977b storm (Fig. 1). Viking Lander 1 continues to operate and may transmit surface pressure data as late as 1994. If so, the data will provide a unique record of the episodic great dust storms on Mars.

R. W. ZUREK
Jet Propulsion Laboratory, California Institute of Technology, Pasadena 91109

C. B. LEOVY
Department of Atmospheric Sciences, University of Washington, Seattle 98195

References and Notes

1. C. B. Leovy, *J. Atmos. Sci.* **38**, 30 (1981).
2. R. W. Zurek, *Icarus* **45**, 202 (1981).
3. If the scattering is isotropic, $g_a = 0$, but if it is all in the forward direction, $g_a = 1.0$.
4. J. B. Pollack, D. S. Colburn, F. M. Flasar, R. Kahn, C. E. Carlston, D. Pidek, *J. Geophys. Res.* **84**, 2929 (1979).
5. C. B. Leovy and R. W. Zurek, *ibid.*, p. 2956.
6. B. J. Conrath, *J. Atmos. Sci.* **33**, 2430 (1976).
7. R. W. Zurek, *ibid.*, p. 321.
8. For a general review of classical atmospheric tidal theory, see S. Chapman and R. S. Lindzen, *Atmospheric Tides* (Reidel, Hingham, Mass., 1970), pp. 106–169.
9. G. A. Briggs, W. A. Baum, J. R. Barnes, *J. Geophys. Res.* **84**, 2795 (1979); A. R. Peterfreund and H. H. Kieffer, *ibid.*, p. 2853.
10. R. S. Lindzen, *J. Atmos. Sci.* **27**, 536 (1970).
11. This is Jet Propulsion Laboratory Atmospheres Publication 980-21 and Contribution 584 from the Department of Atmospheric Science, University of Washington. Work by R.W.Z. represents one phase of research carried out at the Jet Propulsion Laboratory under NASA contract NAS 7-100. Supported by the Planetary Atmospheres Program Office, Office of Space Sciences, National Aeronautics and Space Administration.

9 January 1981; revised 6 April 1981

Circular Feature Among Dunes of the Great Sand Sea, Egypt

Abstract. *A circular crater, about 4 kilometers in diameter and located at 24.2°N, 26.4°E, was discovered in Landsat images among the linear dunes of the Great Sand Sea, Egypt. The crater has a sharp and crenulated rim crest, a terraced wall, a discontinuous inner structure (approximately 1.6 kilometers in diameter), and a few rim blocks. Its morphological and morphometric characteristics are similar to those of meteorite impact craters and other circular structures on the moon and the terrestrial planets. Because of its interaction with windblown sand, it is particularly comparable with craters on Mars.*

The Western Desert of Egypt has been the site of much of the basic research on dune classification and sand movement by the wind (*1*). It is part of the eastern Sahara, the driest large expanse of land on Earth, where received solar radiation is capable of evaporating 200 times the amount of rainfall (*2*). This vegetation-free, north-dipping plain of sedimentary rocks is crossed by numerous belts of sand dunes predominantly of the linear type; the largest accumulation of such dunes forms the Great Sand Sea (Fig. 1) (*1*).

The southern part of the Western Desert was recently divided into two physiographic provinces, the Arba'in Desert in the east (*3*) and the Uweinat Desert in the west (*4*). The Arba'in Desert was named after the Darb El-Arba'in camel track that connects the Kharga Oasis in Egypt to El-Fasher in the Sudan. It contains numerous Paleolithic and Neolithic sites, which indicate episodic human habitation from 200,000 to 5000 years ago (*3*). Similar indications of former pluvial phases exist in the Uweinat Desert, which was named after the 35 by 20 km, 600-m-high mountain at the intersection of the borders of Egypt, Libya, and the Sudan (*4*).

Fluvial action in the geological past, followed by eolian activity under the extremely arid conditions of today, have produced a landscape in the Uweinat Desert that is comparable to that of

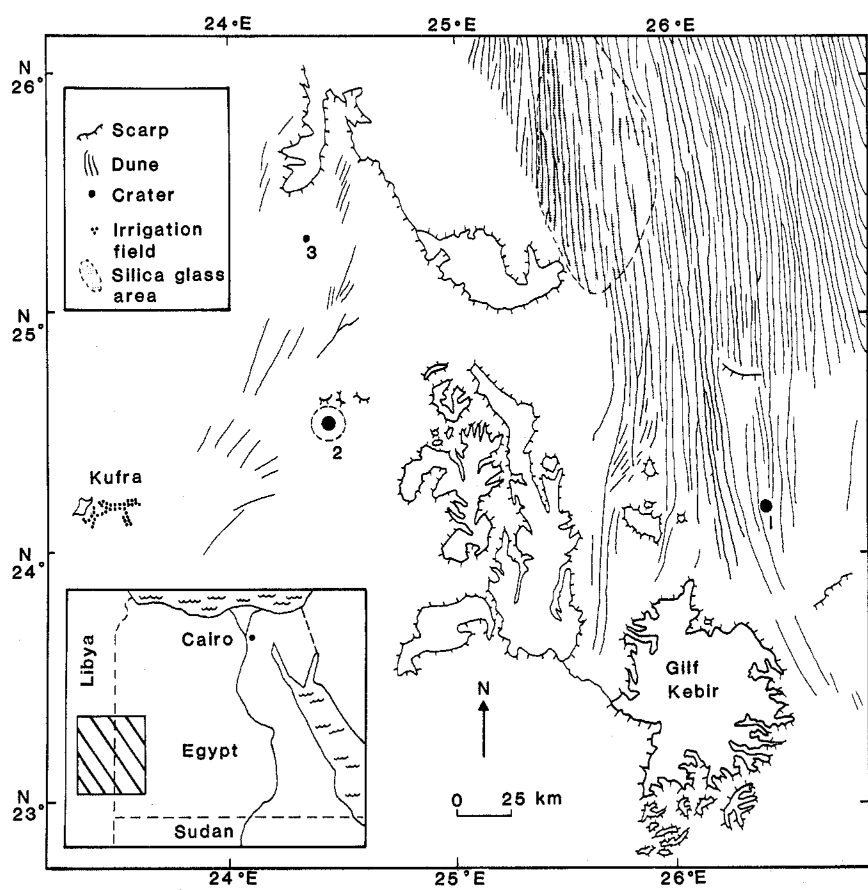

Fig. 1. Map showing the southwestern termination of the Great Sand Sea (upper right), north of the Gil Kebir plateau. Numbered dots are El-Baz Crater (site 1) and two craters, believed to be the result of meteorite impacts, named Oasis Astrobleme (site 2) and BP (British Petroleum) structure (site 3).

0036-8075/81/0724-0439$00.50/0

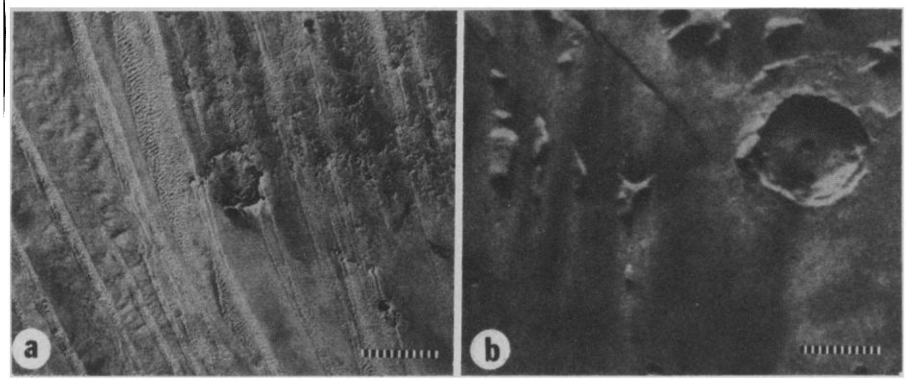

Fig. 2. (a) Landsat view of El-Baz Crater (scale bar, 5 km). (b) Viking Orbiter view of a crater in the Cerberus region of Mars with a dark patch on the leeward side (scale bar, 20 km).

Mars. Canyons and wind streaks revealed on Mars by Mariner 9, Viking 1, and Viking 2 resemble features in the Uweinat area photographed by the Apollo-Soyuz astronauts and Landsat (*5*).

The most imposing features of the Uweinat Desert are the linear dunes of the Great Sand Sea. This sand sea covers an area the size of Ireland—over 72,000 km^2. Individual dunes are often over 100 km long and 100 m high. The base of each dune, 2 km wide on the average, is usually a gently sloping, relatively stable whaleback dune. The whalebacks are commonly topped by sharp-crested, constantly shifting seif dunes.

Another significant feature of the Uweinat Desert is the abundance of crater forms. Most of these craters are believed to be of volcanic origin, such as the Clayton craters, a field of some 20 (*6*). Furthermore, four subdued circular features approximately 130 km east-southeast of Uweinat Mountain and up to 14 km in diameter were revealed by Landsat images. These features, named Bagnold, Miskin, Shaw, and Sweeting after the explorers whose tracks came nearest to them (*6*), have not yet been studied in detail and remain of unknown origin.

A circular feature was discovered among the dunes of the Great Sand Sea on Landsat multispectral scanner frame 10113-08135 and return beam vidicon frame 30960-07490 (site 1 in Fig. 1; Fig. 2a). It is located at 24.2°N, 26.4°E in sandstone of the Nubia series, which covers most of the southern part of the Western Desert. This crater is about 4 km in diameter, being 3.8 km across in one place and 4.2 km at the protrusion on the southeast corner. It has a complex structure with a flat floor, a terraced wall, a crenulated rim, and the subdued remains of an inner structure, approximately 1.6 km in diameter, that may have been a central uplift. The crater is surrounded by a rough-textured deposit, particularly on the east side. This deposit, which contains large blocks, extends up to 2 km from the rim.

The morphological characteristics of the crater are similar to those of craters produced by meteorite impact (*7*). Its outline is similar to that of the bowl-shaped (1.2 km in diameter) Barringer (Meteor) Crater in northern Arizona (*4*). However, the feature in the Western Desert may have formed by a circular diorite intrusion; after erosion by the wind only the hardened and metamorphosed sandstone would remain to form the circular crater (*8*).

Shadow measurements show that the crater is less than 100 m deep. However, because of its location in the path of sand-carrying winds, much of the original shape could have been modified. Also, the southwestern corner of its rim appears to have been eroded and partly buried by a sand dune (Fig. 2a). Because of the lack of named features in the crater's vicinity, I will use the prerogative of the discoverer and name it El-Baz Crater.

El-Baz Crater shows similarities to flat-floored craters in the lunar highlands and on Mercury. It shows even more similarities to martian craters because of its interaction with a strong wind regime in an arid environment. Of special significance are the protrusion on the crater's southeast corner and the crenulated rim, the deflection of dunes by the crater rim and the occurrence of a sand-free zone in its lee, and the dark splotch just south of the rim in the lee of the wind. All three features are common on martian craters (*5*), particularly in the Cerberus region (Fig. 2b). Because of this, an expedition will be organized to collect samples and to study the crater's morphology and interaction with the wind regime of the Great Sand Sea.

FAROUK EL-BAZ

National Air and Space Museum, Smithsonian Institution, Washington, D.C. 20560

References and Notes

1. R. A. Bagnold, *Geogr. J.* **82**, 103 (1933); *The Physics of Blown Sand and Desert Dunes* (Methuen, London, 1941).
2. D. Henning and H. Flohn, *Climate Aridity Index Map* (United Nations Conference on Desertification, Nairobi, Kenya, 1977).
3. C. V. Haynes, *NASA Tech. Memo.*, in press.
4. F. El-Baz, *Lunar Planet. Sci.* **12**, 251 (1981).
5. ——, *Astronaut Observations from the Apollo-Soyuz Mission* (Smithsonian Institution, Washington, D.C., 1977), pp. 76–80; —— and T. A. Maxwell, *Proceedings of the Tenth Lunar and Planetary Science Conference* (Pergamon, New York, 1979), pp. 3017–3030; F. El-Baz, C. S. Breed, M. J. Grolier, J. F. McCauley, *J. Geophys. Res.* **84**, 8205 (1979); J. F. McCauley, C. S. Breed, F. El-Baz, M. I. Whitney, M. J. Grolier, A. W. Ward, *ibid.*, p. 8222; F. El-Baz *et al.*, *Geogr. J.* **146**, 51 (1980).
6. R. A. Bagnold, *Geogr. J.* **93**, 281 (1939); F. El-Baz and B. Issawi, *NASA Tech. Memo.*, in press.
7. M. R. Dence, *Ann. N.Y. Acad. Sci.* **123**, 941 (1965).
8. C. V. Haynes, personal communication.
9. Supported by NASA grant NSG-7188. I thank R. F. Fudali and D. J. Milton for reviewing the manuscript.

10 March 1981; revised 8 May 1981

Man-Made Radionuclides Confirm Rapid Burial of Kepone in James River Sediments

Abstract. *Profiles of man-made radionuclides in sediment cores from the James River estuary confirm the rapid burial of the pesticide Kepone. The greatest deposition of Kepone has occurred in zones characterized by very high sedimentation rates, 10 to 20 centimeters per year. Since sediment is the major Kepone reservoir, rapid burial probably reduces the exposure of organisms to further contamination. Disturbance caused by hurricanes or dredging, however, could return highly contaminated sediment to the surface although this sediment would be diluted with less contaminated particles.*

Estuaries are accumulation sites, at least in the short run, for many of the "lost" or discarded by-products of man's activities. Contaminants, such as heavy metals, radionuclides, or organic chemicals, which become associated with fine-grained sediment, are deposited in estuaries where river currents slacken and salinity-induced flocculation occurs. Simpson *et al.* (*1*) demonstrated that man-made radionuclides in the Hudson River estuary serve as useful indica-

0036-8075/81/0724-0440$00.50/0